AC Calorimetric Design for Dynamic Heat Capacity of Biological Materials

Shigeo Imaizumi*
Nara University, Faculty of Sociology

1 INTRODUCTION

We developed a new AC calorimeter for the measurement of dynamic specific heat capacity in liquids, including aqueous suspensions of biological materials. This method has several advantages. The first is that a high-resolution measurement of heat capacity, in milli-degrees, can be performed as a function of temperature, even with a very small sample. Therefore, AC calorimeter is a powerful tool to study critical behavior at phase transition in biological materials.

The second advantage is that the dynamic heat capacity can be measured. We have interest in the frequency dependence of the heat capacity.

The third advantage is that the sensitivity of detecting an anomaly in the heat capacity is quite high, an amount of the sample can be very small, and it is easy to measure the heat capacity precisely. Using this AC calorimeter we performed the measurements of dynamic specific heat capacity of a lipids suspended in water.

In next paragragh, an experimental method in AC calorimeter for biological materials is discussed. We describe the two types of AC calorimeter, in which thermal energy is supplied either by the irradiation of alternately-chopped light or by AC Joule-heating. Using this direct Joule-heating AC calorimeter we carried out AC calorimetric studies at a very low frequency.

2. EXPERIMENTAL METHOD FOR MEASURING DYNAMIC HEAT CAPACITY

This paragragh describe the AC calorimetry technique used in measuring the heat capacity of phospholipids, the system used for data acquisition, and the sample cells. The theory of AC calorimetry has been discussed in many papers[1)2)3)] ; hence, only a brief review will be mentioned below.

*Received September14, 2005. The Professor, Faculty of Sociology, Department of Contemporary Sociology

2・1 AC Heat Capacity

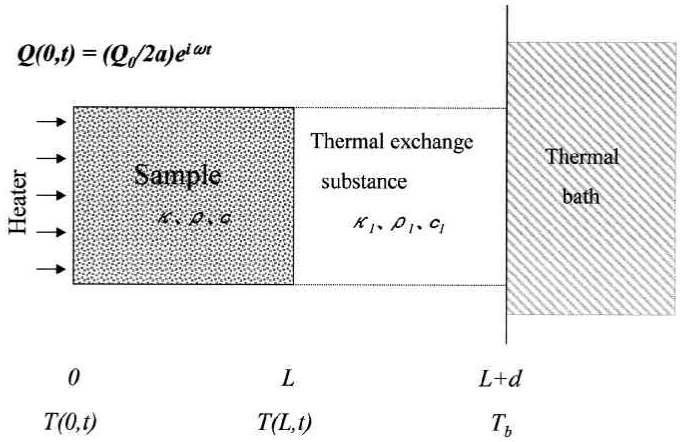

Fig.1

One-dimensional thermal system in an AC calorimetry technique for the case of a sample with thermal conductivity. $q(0,t)$ is the heat flux. κ、c and ρ are the thermal conductivity of the sample, its specific heat and its density. κ_1, c_1 and ρ_1 are the thermal conductivity of the thermal exchange substance, its specific heat and its density, respectively. L and d are thickness of the sample and the thermal exchange substance, respectively.

The schematic diagram of an AC calorimeter is shown in Fig.1. A sample, in the form of a slab of thickness L and cross-section area a, is heated uniformly at one side $(x=0)$ by applying a sinusoidal heat flux $q(0,t)=(Q/2a)e^{i\omega t}$. The other side of the slab $(x=L)$ is coupled uniformly to a bath at constant temperature T_b through the thermal exchange substance. Let the thermal conductivity of the sample be κ, its specific heat c, and its density ρ. Then the thermal diffusivity n is defined by the relation $n=\kappa/\rho c$. The characteristic length $l_0=\sqrt{2n/\omega}$ and its reciprocal $k=1/l_0$ are also introduced. To find the AC temperature in the materials as a function of x and t, the heat conduction equation was solved with proper boundary conditions[1]. The heat conduction equation is

$$\partial T/\partial t = \kappa/\rho c \cdot \partial^2 T/\partial x^2 = n \cdot \partial^2 T/\partial x^2 \qquad (1)$$

The proper boundary conditions come from the requirements that $T_{(x=L+d)} = T_b$ for all t. The condition is as follows :

$$-\kappa a \cdot \partial T/\partial x|_{x=0} = (Q_0/2a)e^{i\omega t}$$

and

$$\kappa a \cdot \partial T/\partial x|_{x=L+} = \kappa_1 a \cdot \partial T/\partial x|_{x=L-} \qquad (2)$$

All quantities are supposed to be multiplied by a time-factor $exp(i\omega t)$, which is omitted throughout and only included at the end of the calculation if real or imaginary parts have to be taken into account. At each point we shall always to interested in two quantities ; $T(x,t)$, $q(x,t)$ $(=q(x)e^{i\omega t})$. They are the temperature and flux at point x, respectively. Then, the general solution corresponding to be the steady periodic conditions, omitting the time-factor, is given by the equation

$$T(x)=M\sinh[k(x-x_1)(1+i)] + N\cosh[k(x-x_1)(1+i)], \tag{3}$$

$$Q(x)=-\kappa k(1+i)\{M\cosh[k(x-x_1)(1+i)] + N\sinh[k(x-x_1)]\times(1+i)]\}. \tag{4}$$

where

$$k = \sqrt{\omega/2n}, \tag{5}$$

M and N are constants.

Let $T(x_1)$ and $q(x_1)$ be the temperature and flux, respectively, at face $x=x_1$ of the slab and let $T(x_2)$ and $q(x_2)$ be their values at face $x=x_2$. If any two of these four quantities are given, M and N can be determined from them, Thus the set of $T(x_1)$, $q(x_1)$ *or* $T(x_2)$, $q(x_2)$ can be expressed in terms of the original two.

By the application of the matrix element, the oscillatory temperature dependence of the sample at the rear surface is found to be

$$T_{ac}(L) = (Q_0R_1/2a)e^{i\omega t}/\{k_1d(1+i)\coth[k_1d(1+i)]\cosh[kL(1+i)] + R_1\kappa k(1+i)\sinh[kL(1+i)]\} \tag{6}$$

where $k=(\omega/2n)^{1/2}=(\omega\rho c/2\kappa)^{1/2}$, $k_1=(\omega\rho_1c_1/2\kappa)^{1/2}$ *and* $R_1=d/\kappa_1$.

When $c_1 \to 0$, namely $k_1 \to 0$,

$$T_{ac}(L) = (Q_0R_1/2a)e^{i\omega t}/\{\cosh[kL(1+i)]+R_1\kappa k(1+i)\sinh[kL(1+i)]. \tag{7}$$

Under the conditions that $\omega\tau_s=2\kappa k^2La/R_1>>1$ and that the sample dimension L is smaller than the characteristic thermal length l_0 ; that is,

$$kL << 1,$$

the temperature variation can be expressed as

$$T_{ac}(L) = (Q_0R_1/2a)e^{i\omega t}/\langle\{1+[kL(1+i)^2]/2!+[kL(1+i)]^4/4!+ \cdots\}$$
$$+R_1\kappa k(1+i)\{[kL(1+i)+[kL(1+i)^3/3!+[kL(1+i)]^5/5!+ \cdots]\rangle$$

Then, the AC temperature and the phase are approximately given by

$$T_{ac}(L) = (Q_0/2a)e^{i(\omega t-a)}/2\kappa k^2L\{1+1/(2\kappa k^2LR_1)^2+2k^4L^4/45+2L/3R_1\kappa\}^{1/2}, \quad (9)$$

$$a = \arcsin\langle[1+L/2R_1\kappa-k^4L^4]/[1+1/(2\kappa k^2LR_1)^2+2k^4L^4/45+2L/3R_1\kappa]\rangle. \quad (10)$$

Putting

$$\tau_s = c\rho LR_1 \quad (11)$$

and

$$\tau_{int}=L^2/\sqrt{90n.} \quad (12)$$

Tac becomes

$$T_{ac}(L) = Q_0/2\omega C_s\times[1+(1/\omega^2\tau_s^2)+\omega^2\tau_{int}^2+(2L/3R_1\kappa)]^{-1/2}\times e^{i(\omega t-a)}, \quad (13)$$

$$a = \arcsin\langle[1-(4\omega^2\tau_{int}^2/3)+(L/3R_1\kappa)]/[1+(1/\omega^2\tau_s^2)+\omega^2\tau_{int}^2+(2L/3R_1\kappa)]\rangle, \quad (14)$$

where $C_s = c\rho La$.

In these expressions, τ_s is the sample-to-bath relaxation time, τ_{int} is relaxation time for thermal equilibrium in the sample and C_s is the heat capacity of the sample. When ω is chosen so that $1/\tau_s<<\omega<<1/\tau_{int}$, the frequency-dependent term in Eq. (13) is expressed by

$$C_s = Q_0/2\omega T_{ac}(L) \quad (15)$$

$$a = \pi/2. \quad (16)$$

where Q_0 is the value of the AC input power, $\omega=2\pi f$ and T_{ac} are the frequency and the AC amplitude of the resulting temperature oscillations, respectively. Therefore, the heat

capacity is inversely proportional to the amplitude of the AC temperature.

2. 2 The Design of AC Calorimeters

We will discuss an apparatus for liquid including suspension of biological materials in the temperature range between 170 and 400 K.[5]

The AC calorimetry methods may be characterized by the AC heat sources : One method involves the use of irradiation by alternately chopped light, and another method is to use direct Joule-heating of a substance with electrical resistance that has been attached to a sample. Both methods have advantages. We used the second method in our experiments, and we performed the measurement of heat capacity at the main phase transition of a lipid suspended in water.

2. 2. 1 AC Calorimeter Using Chopped-Light Irradiation

Figure 2 is a diagram of the measuring system of the AC calorimeter. The thermal energy was periodically supplied to the bottom of the sample cell by chopped light from a halogen lamp (Ushio Electric Inc., Type JC-12V-50W). The AC temperature (T_{ac}) was detected by two pairs of chromel-alumel thermocouple wires with 0.025-mm diameter (supplied from Omega Engineering Inc.), which were glued to a sample cell. The AC temperature was detected by one of the thermocouples and read by a lock-in amplifier (Princeton Applied Research Inc., Model 124A) with the reference signal from the chopped light. Another thermocouple was used to measure the increments of the DC temperature (hereafter indicated as T_{dc}) beyond the temperature of the thermal bath. The temperature of the thermal bath (hereafter indicated as T_b) was measured by a calibrated platinum-resistance thermometer (Rosemount Engineering Co., Model 118MF). Therefore, the actual temperature of the sample is given by T_b+T_{dc}. A linear relation between $1/T_{ac}$ and the total heat capacity is required for AC heat capacity measurement. To test the linear relation, there are two ways, as discussed in the following. Both the amplitude and the phase are expressed in terms of the similar functions of τ_s and τ_{int} as given in eqs.(13) and (14).[6] Under the above conditions, the inverse of the amplitude is proportional to the total heat capacity and at the same time the phase is equal to $\pi/2$. One way, then, is the amplitude-examination method, to test whether the amplitude is inversely proportional to the frequency. The other way is the phase-examination method, in which the phase is kept constant, at $\pi/2$, in the actual measurement.[3] The latter method was used in the experiment. It is worthwhile noting that the phase shift can be detected with a high resolution by means of a lock-in amplifier.

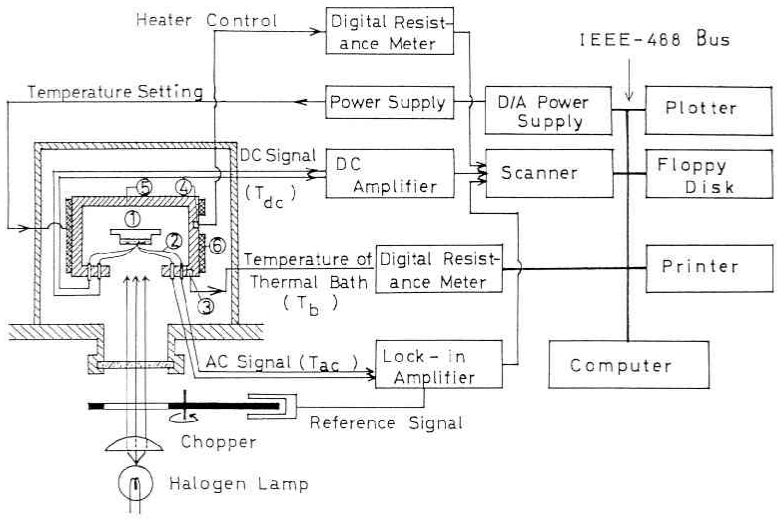

Fig.2

Schematic diagram of the chopped-light irradiation-type measuring system. The AC temperature response of the sample, T_{ac}, is inversely proportional to the heat capacity, C_s, as given by $C_s = Q_0/2\omega T_{ac}$, where Q_0 is the amplitude of the input thermal energy. ω stands for $2\pi f$. In our measurements all of the data processing and control were performed by means of a personal computer.

1 : sample cell, 2 : thermocouple, 3 : platinum thermometer for the temperature measurement of a thermal bath, 4 : platinum thermometer for temperature control, 5 : thermal bath, 6 : heater.

We developed a computer-controlled AC calorimeter. All the measurements were taken using a personal computer (Commodore, Type CBM 3032) with an IEEE-bus. Finally, the data were automatically printed out and the results were also simultaneously plotted against temperature on a XY plotter. The temperature of the thermal bath was changed stepwise. The temperature step ΔT was set by a software program. At each temperature the temperature of the thermal bath was kept constant for a period Δt, also set by the software program. During the constant-temperature, period one point of the data was obtained at a temperature. Therefore, the results obtained by AC calorimetry exhibit steady values and do not depend on ΔT and Δt. When the temperature is held constant, the value of the observed heat capacity does not change for the period Δt. On the other hand, in the case of differential scanning calorimetry (DSC), the temperature is scanned continuously. Then, the lag of temperature change is integrated subsequently and, as a result, the curve of heat capacity depends on the scanning rate.

In the present experiment the scattering of the data was smaller than 0.2% of the heat capacity.

2. 2. 2 AC Calorimeter Using Joule-Heating

The heat capacity is well described by the sample expression

$$C_p = Q_0/\omega \Delta T_{ac}\,, \tag{17}$$

Where Q_0 is the amplitude of the AC power input from the microfilm heater, $\omega=2\pi f$ and ΔT_{ac} are the frequency and the zero-to-peak amplitude of the resulting temperature oscillations, respectively.[6,7,8]

The electronic system used for this experiment is shown schematically in Fig.3. The calorimetry was operated at a constant frequency ω = 0.196 sec^{-1}, which corresponds to a 32 sec period for the temperature oscillations. A multiplexer was used to measure successively the heater power, the resistance of a platinum thermometer, and the thermistor resistance at every 0.5 sec during eight period of oscillation. A typical ΔT_{ac} temperature amplitude of ±5 mK corresponds to a resistance variation of $\Delta R \fallingdotseq 60\ \Omega$ for a thermistor with R=70 k Ω. The Keithley 192 digital voltmeter used for this measurement is capable of 6.5 decades of resolution, and the scatter of the C_p values is smaller than 0.2 %. The output of the oscillator and the resistance of the thermistor are read simultaneously by the microcomputer, which allows us to get the amplitude ΔT_{ac} and the phase $\Phi = tan^{-1}(-\omega \times C_p/K)$, where K is the thermal conductance between the sample and the thermal bath. The data are corrected for drift by averaging the temperature of the sample over the duration of the measurement, as follows : The output of the thermistor reading that corresponds to the zero crossing of the heater input is taken, and thus obtained drift part is subtracted from the data set of the output of the thermistor reading.

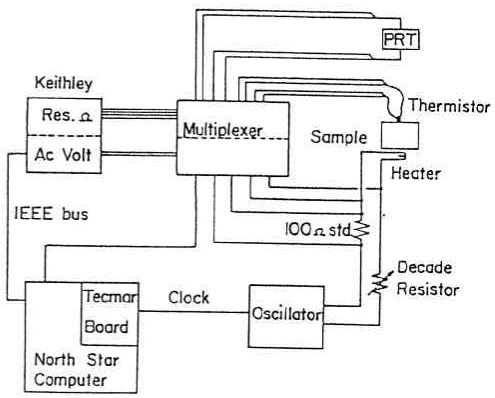

Fig.3

Block diagram of the electronics for the Joule-heating type AC calorimetric experiment. The resistance of a platinum resistance thermometer (PRT) and a thermistor are read with a four terminal wires measurement. The voltage is read with a two terminal wires measurement.

2. 2. 3 The Design of a Sample Cell

The sample cell for Joule-heating type measuring system is shown in Fig. 4. The body of the cell is a cup, 10 mm in diameter and 1.2 mm in depth, pressed from a 0.25 mm silver sheet. A lid of 0.075 mm silver foil is attached to the sample cell, using a cold-welded indium seal. A long coil of a fine gold wire was inserted into the cell to increase the effective internal thermal conductivity. The AC heat input is supplied by a thin film resistance heater, and the resulting temperature oscillations (T_{ac}) are measured with a microbead thermistor.

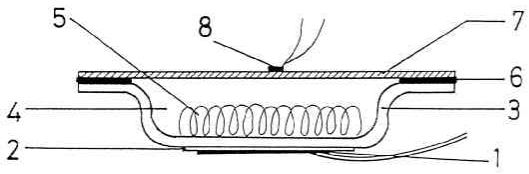

Fig.4

A sample cell for sample of liquid suspension.
1. Microfilm heater. 2. Varnish layer.
3. Silver cup. 4. Sample
5. A long coil of fine gold wire.
6. Indium seal. 7. Silver lid. 8. Bead thermister.

One was able to assess the weight of all the materials involved in the construction of the sample cell. Table 1 presents a list of these materials with their respective weights in a typical cell with a final weight of about 600 mg. The heat capacity of the empty cell was determined as follows: After finishing all the measurements on the filled cell, a small hole was made in the lid of the cell and most of the suspension was withdrawn with a syringe.

Table 1

Wight and heat capacity of the materials used in constructing a sample cell.

Material	Weight (g)	Heat capacity (J/K) *
Silver	0.3848	0.0913
Indium	0.0503	0.0119
Gold wire	0.0335	0.0043
Heater	0.0015	0.0019
Copper (1/3 of the length is estimated to be a part of the cell)	0.0126	0.0048
Epoxy	0.0387	0.0404
Sample	0.0958	
Total for filled cell	0.6229	
Contribution from empty cell	0.5214	0.155

* Values given at 300 K.

The cell was then rinsed with water and placed in a drying oven at about 340 K for three hours to completely evaporate any residual suspension. The empty cell was weighed and its heat capacity was measured over the same temperature range as that for studying the filled cell.

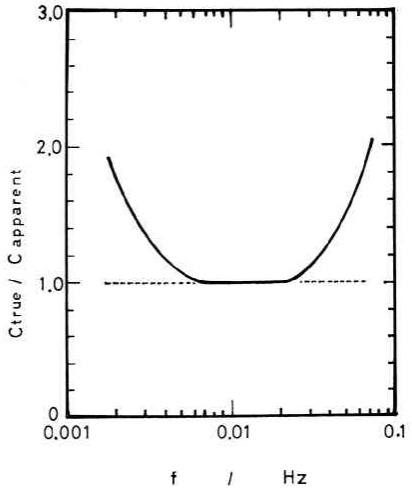

Fig.5
The AC heat capacity of a water sample as a function of frequency.

Besides we considered whether the conditions of AC heat capacity measurement were satisfied. In our computer simulations we worked with a water sample, using equation (6). The simulation was run with water of $\kappa = 5.82 \times 10^{-3}$ J · cm^{-1} · s^{-1} · K^{-1}, $\rho = 0.9982$ g · cm^{-3}, c=4.1816 J · g^{-1} · K^{-1} and air of $\kappa_1 = 2.50 \times 10^{-4}$ J · cm^{-1} · s^{-1} · K^{-1}, $\rho_1 = 1.205 \times 10^{-3}$ g · cm^{-3}, $c_1 = 1.006$ J · g^{-1} · K^{-1}, respectively. In Figure 5 we show the specific heat as a function of frequency. At a frequency of 0.03 Hz, the condition for the heat capacity measurement is satisfied, that is, the ratio $C_{ture}/C_{apparent}$ is unity. We see that the data taken in the condition are quite rational.

3 HEAT CAPACITY OF PHOSPHLIPID BILAYERS

Aqueous suspensions of dipalmitoylphosphatidylcholine (DPPC) undergo successive phase transitions involving the structural change of the lipid bilayers. AC calorimetry experiments have been carried out in studying of phase transition of a lipid suspension. In the study, the anomaly of heat capacity has been observed at the main transition. On the basis of the results, we show that there exists a frequency dispersion of the heat capacity.

3．1 Experimental Results by AC Calorimetric Measurement

L-DPPC used in the Joule-heating type AC calorimeter with a very low frequency of 0.03 Hz[10] were obtained from Calbiochem-Behring and Sigma Chemical Co. All materials were found to be sufficiently pure by thin-layer chromatography and were used without further purification.

For the preparation of multibilayer samples, lipids were weighted out and dissolved in spectroscopic-grade chloroform. The samples were dried under purified nitrogen gas and

then kept under vacuum for at least one hour to achieve complete dryness. Then, distilled water was added to the dried samples and the mixture was shaken to disperse the lipid-water mixtures. The suspensions were degassed and heated up to the transition temperature for about one day to obtain uniform suspension. Samples of the DPPC (Calbiochem.) /water and DPPC (Sigma) /water systems were prepared with lipid contents of 6.25wt% and 15.0wt%, respectively.

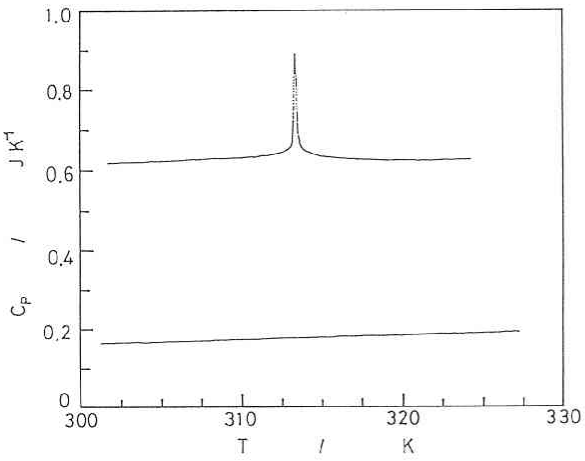

Fig.6

The heat capacity of a filled cell containing 0.0958 g of DPPC suspension (upper curve) and the empty cell (lower curve). DPPC (Calbiochem.) at 6.25 wt% was scanned at 0.12 K/h on heating.

The upper curve in Fig. 6 shows the total heat capacity of the DPPC suspensions, including that of the silver cell.[9] The lower curve shows the heat capacity for the empty cell. The measured C_p values, $C_p(obs.)$, correspond to the total heat capacity of a sealed cell weighing about 620 mg, of which 90-100 mg is the weight of the DPPC suspensions.[9] The values of the heat capacity per gram of DPPC are determined from

$$C_p = [C_p(obs.) - C_p(empty)] / W, \tag{18}$$

where W is the weight of DPPC in the suspension.[11] The empty cell data is well described by a straight line :

$$C_p(empty) = 1.295 \times 10^{-3} \cdot T - 0.231 \ (J/K), \tag{19}$$

which was obtained by a least-squares fit to 276 points over the temperature range of 300 – 325 K. Thus the measured heat capacity of the empty cell, $C_p(empty)$, varies linearly from 0.158 J/K at 300 K to 0.190 J/K at 325 K. Using eqs. (18) and (19), one can convert the data points shown in Fig.7 into the heat capacity per gram of DPPC. Note that the small thermal anomaly observed by DSC at the pretransition temperature of 306 K is completely absent from these AC measurement at 0.6 Hz.[5,10]

Figure 8 display the temperature dependence of the excess heat capacity per gram of DPPC measured in multilamellar aqueous suspensions, whose concentration was 6.25 wt% of

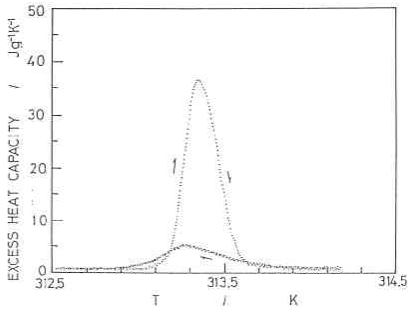

Fig.7

Calorimetric phase transition curve for DPPC (Calbiochem.). DPPC at content of 6.25 wt% was scanned at 0.12 K/h. The excess apparent specific heat is plotted against the temperature, with the maximum occurring at 313.36 K on heating. The AC heat energy was supplied at a frequency of 0.03 Hz.

DPPC. This excess heat capacity corresponds to the quantity $C_p - C_p(background)$, where C_p ($background$) represents the normal heat capacity obtained.

On cooling, the excess heat capacities associated with the transition are substantially smaller than those obtained heating. Thus these AC calorimetry results with a frequency of 0.03 Hz indicate irreversibility at the main transition. Recently, the reversibilities in the phase transition were studied by Yao et al.[11] in DPPC bilayers, using small angle X-ray scattering and freeze-fracture electron microscopy. They have reported that the main transition of DPPC is not reversible in the sense that the initial P_β' phase, appearing on heating from the L_β' phase, does not reappear on cooling from the L_β' phase, but is replaced by a metastable phase P_β' (mst). The excess C_p peaks 0.6 Hz on heating were smaller than those obtained here on heating.

The areas under the excess C_p curves shown in Fig. 8 for heating runs are 5.674 kJ/mol. The corresponding areas for cooling runs are 1.293 kJ/mol. These values are all much smaller than the latent heat ΔH = 35.6 kJ/mol obtained with a DC method and high-sensitivity DSC or ΔH = 38.8 kJ/mol obtained with an adiabatic calorimeter.

The area of the excess heat capacity peak obtained from AC heating measurements at 0.03 Hz is only about one-sixth of ΔH ;and, furthermore, the peak is smaller for AC measurements at 0.6 Hz, where the area under the excess C_p curve is 3.19 kJ/mol for heating run.[5] In the above experiment, the linear scan rate is 0.12 K/h = 0.033 mK/sec. Since the AC temperature oscillation are typically 10 mK peak-to-peak over a half period of 16 sec, the average rate of variation in AC heating is ~0.63mK/sec (or roughly 20 times greater than the scan rate). In the case of AC measurements at 0.6 Hz, the corresponding variation in AC heating is

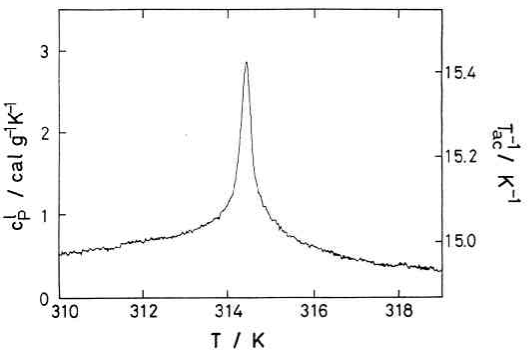

Fig.8

Temperature dependence of the excess heat capacity.

~12.5 mK/sec over a half period of 0.8 sec. relatively fast time scale of t ≦0.8 sec, the phase shift is almost constant. There is a marked difference in the behavior observed on heating and cooling. It would be interesting to study the frequency dependence of the excess heat capacity.

The concept of dynamic heat capacity has already been used. Kummer et al.[12] have first pointed out that time-dependent specific heat takes place in amorphous SiO_2, which is interpreted in terms of the tunneling model. In studies of elastic dispersion, the relaxation strength is expressed by dynamic heat capacity, and also, its relaxation time is related to the dynamic heat capacity. Especially in the study of ultrasonic attenuation at the transition temperature, the concept of dynamic heat capacity has been used in order to analyze the result. To establish this concept further, we expect to observe directly the frequency dispersion of heat capacity by AC calorimetry. The transition enthalpies were obtained by measureing the areas of the excess heat capacity peak with a digital planimeter (Planix7). These values are shown as a function of the frequencies in Fig. 9. For example, the enthalpy obtained by an adiabatic calorimeter is 38.8 kJ/mol, while the integrated area of the excess heat capacity peak obtained by an AC method at 0.03 Hz is at most 6.4 kJ/mol.[10] These facts indicate that there exists a quite slow relaxation process during the main transition and, therefore, it means that there exists a large frequency dispersion of the heat capacity in this frequency region.

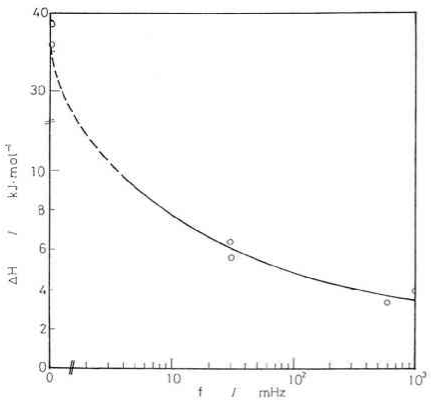

Fig.9

Frequencies dependence of the dynamic enthalpies in DPPC

4. DISCUSSION AND CONCLUSIONS

The result obtained by AC calorimetry provides clear evidence that the heat capacity anomaly due to the fluctuation of order parameter takes place at the phase transition. The sharp peak strongly suggests that the fluctuation of order parameter takes place at the main transition (T_m). The pseudo-critical heat capacity will tentatively be analyzed in terms of critical-exponent expressions.

As shown in Fig. 8, the heat capacity of DPPC clearly indicates a divergence. This result was tentatively analyzed in terms of a usual critical-exponent expression for heat capacity as

$$C_p = A|t|^{-\alpha} + B + Et, \qquad t = (T - T_{m1})/T_{m1}, \tag{20}$$

for $T>T_m$, α is so-called critical exponent, which should be called pseudo-critical exponent. A is pseudo-critical amplitude, B is constant background and E is the slope of the background. For $T<T_m$, we used primed parameters, α', A', B', E' and $t=(T_{m2} - T)/T_{m2}$. In the following analysis, we assumed that $E=E'=34.2\ J \cdot g^{-1} \cdot K^{-1}$ and $T_m=T_{m1}=T_{m2}$.

A least-squares fitting analysis was performed with the use of the SALS program at Nagoya University Computation Center, treating α, α', A, A', B, B' and T_m as adjustable parameters. The best fitted values are listed in Table 2. It was found that both of α and α'

Table 2

Parameters for eq.(20) above T_m and the similar equation below T_m'. The constraints $T_m=T_m'$ and $E=E'=34.2\ J \cdot g^{-1} \cdot K^{-1}$ were imposed.

α	α'	$A / Jg^{-1}K^{-1}$
0.40 ± 0.05	0.4 ± 0.1	0.63 ± 0.25

$A' / Jg^{-1}K^{-1}$	$(B' - B) / Jg^{-1}K^{-1}$	T_m / K
0.23 ± 0.20	3.8 ± 0.4	314.35 ± 0.02

are nearly equal to 0.4 and A and A' are almost identical within uncertainty. This result provides insight into pseudo-behavior. The value of α and α' is 0.5, rather close to that in the three dimensional Gaussian model. However, the pseudo-critical behavior in this case should be considered in terms of the disorder of hydrocarbon chains. It has been calculated on the basis of the theory by Izuyama and Akutsu[13] that the exponent associated with spinodal point is 1/2 and on the other hand, at the critical point the critical exponent becomes 2/3. The system dealt with in the study seems to lie very near the critical point, because $T_m \sim T_{m'}$. However, both of the theoretical exponents are larger than that obtained experimentally.

We describe a high sensitive AC calorimeter based on the irradiation of alternately-chopped light or ac Joule-heating. It is possible to measure heat capacity anomaly due to the pseudo-critical phenomenon. Recently, AC calorimetry is know as a very powerful tool for the characterization of a wide variety of biological materials and their transitions.[14]

REFERENCES

1）I. Hatta and A. Ikushima : Solid State Phys. **5** 471 （1970）.
2）I. Hatta : Calorimetry and Thermometry and Thermal Analysis 1973 Edition.
3）I. Hatta and A. J. Ikushima : Jpn. J. Appl. Phys. **20** 1955 （1981）.
4）H. S. Carslaw and J. C. Jaeger : Conduction of Heat in Solids. （Oxford University Press, London. 1959） 2nd ed., p110.
5）S.Imaizumi, K.Suzuki and I.Hatta : Rev.Sci.Instrum. **54**, 1180 （1983）.
6）G.Sanchez, M.Meichle andC.W.Garland:Phys.Rev. **A28**, 1647（1983）;C.W.Garland:Thermochem.Acta **88**, 127（1985）.
7）G.Sanchez : Ph.D.thesis, Massachusetts Institute of Technology （1983）.
8）G.B.Kasting, K.S.Lushington and C.W.Garland : Phys.Rev. **B22** 321 （1980）.
9） S.Imaizumi and C.W.Garland : J.Phys.Soc.Jpn. **56** 3887 （1987）.
10）I.Hatta, K.Suzuki and S.Imaizumi : J.Phys.Soc.Jpn. **52** 2790 （1983）.
11）H.Yao, S.Matsuoka, B.Tenchov and I.Hatta : Biochem.Biophys.Acta **814** 300 （1985）.
12）R.B.Kummer, R.C.Dynes and V.Narayanamurti : Phy.Rev.Lett. **40** 1187 （1978）.
13）T.Izuyama and Y.Akutsu : J.Phys.Soc.Jpn. **51** 730 （1982）.
14）H.Huth, A.Minakov and C.Schick : Netsu Sokutei **32** 70 （2005）.